Motions in Fluids Caused by Microgravitational Acceleration and Their Modification by Relative Rotation

J. Iwan D. Alexander*
NASA Marshall Space Flight Center, Huntsville, Alabama
and
Charles A. Lundquist†
University of Alabama, Huntsville, Alabama

It has been recognized for some time that large reductions in effective gravity can be achieved aboard an orbital spacecraft. As a consequence, many materials science experiments have been conducted in space in order to minimize or eliminate undesirable effects that might result because of convective motions in fluids driven by buoyancy effects. Of particular interest are the low-frequency accelerations caused by the Earth's gravity gradient field, spacecraft attitude motions, and atmospheric drag, since it is known that these can give rise to sustained fluid motion. In order to gain a limited understanding of the effects of these accelerations, the authors examined their magnitude and orientation and, in particular, have calculated the Stokes' motion of a spherical particle in a fluid for various types of spacecraft attitude motions. In addition, the effect of slowly rotating the experimental system relative to the spacecraft has been assessed. For a restricted set of conditions, it is possible to increase the residence time of the particle in the neighborhood of its initial position.

Nomenclature

Dimensional Variables and Parameters

A = effective cross-sectional area of spacecraft, cm^2
a_0 = initial value of the osculating (semimajor) axis, cm
C_d = aerodynamic drag coefficient
d = length scale for the spacecraft, cm
G_c = gravitational constant, 6.67×10^{-8} dyne-cm^2-g^{-2}
g = 980 cm s^{-2}
M_e = mass of Earth, 5.96×10^{27} g
m_s = mass of spacecraft, g
ng = 10^{-9} g
R = radius of spherical particle, cm
$\tilde{r}_0$ = distance of spacecraft mass center from origin of geocentric frame
$\tilde{S}$ = Stokes' coefficient, s^{-1}; $= 4.5\mu/(\rho_s R^2)$
$\bar{\beta}$ = effective drag coefficient, cm^2-g^{-1}
γ = $G_c M_e$, dyne-cm^2-g^{-1}
μ = viscosity of fluid, dyne-cm^2-s^{-1}
ρ_{atm} = average mass density of atmosphere, g-cm^3
ρ_f = mass density of fluid, g-cm^{-3}
ρ_s = mass density of spherical particle, g-cm^{-3}
ρ_0 = reference atmospheric mass density, g-cm^3
ω_e = rate of rotation of experimental frame relative to spacecraft frame
ω_0 = angular speed for a circular orbit of radius a_0
μg = 10^{-6} g

Nondimensional Variables and Parameters

$a, e, \bar{\omega}$ = osculating elements
A_{KK^*} = rotation of geocentric frame into spacecraft frame
$F^*_{k^*}$ = dimensionless force per unit mass representing Earth's gravitational force
G_{KM} = gravity gradient tensor (spacecraft frame)
$G^*_{K^*M^*}$ = gravity gradient tensor (geocentric frame)
$G_{\alpha\beta}$ = gravity gradient tensor (experimental frame)
p_α = position of origin of spacecraft frame with respect to origin of experimental frame
$q^*_{K^*}$ = position of spacecraft mass center with respect to origin of geocentric inertial frame
$Q_{\alpha\beta}$ = rate of rotation, $= (dR_{\alpha K}/dt)R_{\beta k}$
$r_0(t)$ = distance of spacecraft mass center from origin of geocentric frame
$R_{\alpha K}$ = rotation of spacecraft frame into experimental frame
S = dimensionless Stokes' coefficient, $= \tilde{S}/(\gamma/a_0^3)^{1/2}$
x_α = position of particle with respect to origin of experimental frame
X_K = position of particle with respect to origin of spacecraft frame
$X^*_{K^*}$ = position of particle with respect to origin of geocentric inertial frame
β = dimensionless atmospheric drag coefficient, $= \bar{\beta}\rho_{atm} a_0 \epsilon^{-1}$
δ = buoyancy coefficient (includes added mass effect)
δ_{KM} = identity tensor, $= R_{\alpha K}R_{\alpha M} = A_{KM}A_{PM}$
ϵ = d/a_0
$\dot{\theta}(t)$ = angular speed of spacecraft
$\theta(t)$ = angular position of spacecraft measured with respect to the X_1^* axis of the geocentric coordinates; positive in the direction of motion of the spacecraft
Ω_{KM} = rate of rotation, $= (dA_{KK^*}/dt)A_{MK^*}$

Received Nov. 20, 1986; presented as paper 87-0312 at the AIAA 25th Aerospace Sciences Meeting, Reno, NV, Jan. 12–15, 1987; revision received March 6, 1987.

*Visiting Scientist, University Space Research Association; currently Senior Research Scientist, Center for Microgravity, and Materials Research, University of Alabama, Huntsville, Alabama.
†Director of Research. Member AIAA.

Introduction

THE accelerations experienced within experimental systems aboard orbiting spacecraft are generally low in amplitude but occur over a broad range of frequencies. The importance of an individual component of the total residual

acceleration field will depend on the response of the particular experiment to the amplitude, frequency, and orientation of that component. Of particular concern to materials scientists are low-frequency and steady residual accelerations, since it is known that these can give rise to sustained fluid motion.[1-3] Sources of residual accelerations range from the Earth's gravity gradient tides, spacecraft attitude motions, and atmospheric drag to the higher-frequency "g jitter" caused by machinery vibration, cooling systems, spacecraft vibrations, and ephemeral disturbances such as crew motions and thruster firings.

Recent work[3,4] concerning the response of a particle to accelerations associated with the gravity gradient, atmospheric drag, and spacecraft attitude motions indicates that the nature of the particle motion depends on a number of factors. These include the density difference between the particle and the enveloping medium, the nature of the drag force exerted by that medium on the particle, the initial position of the particle relative to the spacecraft mass center, and the nature of the attitude motions of the spacecraft (i.e., whether the spacecraft undergoes a rigid-body rotation with respect to an inertial frame of reference). For example, a gravity gradient stabilized attitude will result in a quasisteady acceleration perturbed by disturbances that have the frequency of the orbit. For a solar inertial attitude, the acceleration caused by atmospheric drag will vary with the orbital frequency, while the gravity accelerations will vary at twice that frequency.[3,5,6]

In order to improve our understanding of the effects of some of the low-frequency accelerations (for certain types of spacecraft attitude there will be steady accelerations),[3] the Stokes' motion of a spherical particle subject to the effects of the Earth's gravity gradient field, atmospheric drag, and spacecraft attitude motions is examined. In addition, the possibility that the residence time of a particle in a given region of the fluid may be increased by a continuous rotation of the experimental system relative to the spacecraft is investigated as well. It is assumed that the fluid is "spun up" in the sense that were it not for the presence of the particle, the fluid would undergo the same rigid-body rotation as the experimental system, and that local rotation axis is parallel to basic rotation axis of the spacecraft relative to the geocentric frame.

Two basic attitude motions are considered. One involves a continuous rigid-body rotation relative to a geocentric inertial frame. For the other, the orientation of the spacecraft is fixed with respect to the geocentric frame. The former, which would correspond to the gravity gradient stabilized attitude, involves a rotation in the same sense as the motion of the spacecraft, at a rate equal to the angular speed of the spacecraft, about an axis oriented perpendicular to the orbital plane of the spacecraft, and will be referred to as the "radial attitude"; the latter will be termed the "inertial attitude." Figure 1 depicts the nature of these attitude motions.

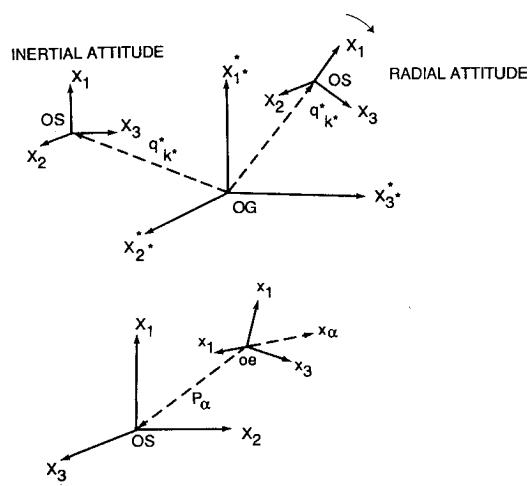

Fig. 1 Frames of reference: oe = origin of experimental frame, OS = origin of the spacecraft frame, OG = origin of geocentric inertial frame.

Table 1 Changes in the gravity gradient acceleration components (in μg/m from the mass center of the spacecraft) for the radial attitude

Altitude, km	$X_{2,3}$	X_1
275	−0.137	0.276
300	−0.136	0.273
325	−0.134	0.27
350	−0.133	0.267
375	−0.131	0.264
400	−0.13	0.261
425	−0.128	0.258
450	−0.127	0.256
500	−0.124	0.25
525	−0.123	0.247
550	−0.121	0.245
575	−0.12	0.242
600	−0.119	0.239

For an experiment aboard a spacecraft in a gravity gradient stabilized attitude, it is found that rotations of the experiment at rates corresponding to twice and one-half the orbital rate can substantially reduce the extent of the particle motion relative to the experimental frame of reference. The most effective rotation (about an axis perpendicular to the orbital plane) appears to be at twice the orbital rate, and in the opposite sense to the direction of motion of the spacecraft.

Dimensionless Variables and Parameters

It is convenient to formulate this problem in terms of nondimensional variables.[3] Distance is scaled using a_0, the initial value of the osculating semimajor axis‡ of the spacecraft orbit, and time is scaled using $(\gamma/a_o^3)^{1/2}$, which physically corresponds to the angular speed, ω_0, of a spacecraft in a circular orbit of radius a_0. An additional length scale d, a characteristic distance within the spacecraft, is also employed to scale distance within the spacecraft.

Gravity Gradient and Atmospheric Drag

Any body capable of motion relative to the spacecraft will be subject to an acceleration relative to the mass center of the spacecraft that arises from the gravity gradient of the Earth. This relative acceleration is the difference between $F^*_{K^*}(X^*_{K^*})$ and $F^*_K(q^*_{K^*})$. It is assumed here that, to a first approximation, only the Earth's gravitational force is important, and interaction between the particle mass and the spacecraft mass is negligible. The force is taken to vary as the inverse square of the distance from the Earth's mass center.

If the distance $\|x^*_{K^*} - q^*_{K^*}\|$ is small compared to unity, then F_{K^*} may be expanded in a Taylor series about q_{K^*}—the position of the mass center of the spacecraft—to give

$$F^*_{K^*}(X^*_{K^*}) = F^*_{K^*}(q^*_{K^*}) + G^*_{K^*M^*}[X^*_{M^*} - q^*_{M^*}]. \quad (1)$$

The term $G^*_{KM^*}$ in Eq. (1) is the gravity gradient.[3,7] Table 1 gives the changes in the gravity gradient acceleration per meter from the spacecraft mass center for a range of altitudes.

A spacecraft is also subject to atmospheric drag.[8] The particle will be subject to an acceleration relative to the spacecraft which is antiparallel to this force. The nondimen-

‡Since the spacecraft is subject to an atmospheric drag force, the spacecraft gradually spirals in toward the Earth. As a result, the orbital elements cannot be defined in the usual sense. The instantaneous values of these elements are referred to as the osculating elements.[8]

sional form of the atmospheric drag acceleration is taken to be[3,5,6,8]

$$F^D_{K^*} = \beta \rho_{\text{atm}} \| \dot{q}^*_{K^*} \| \dot{q}^*_{K^*} \tag{2}$$

where $\beta = \bar{\beta} a_0/\epsilon$, ρ_{atm} varies with the altitude of the spacecraft, and where $(^*)$ denotes a (dimensionless) time derivative. The particular expression used is described by Eq. (6.3) of Ref. 9, and has been employed in previous calculations of this nature.[3,5] Typical values of drag accelerations are given in Table 3.

Centrifugal, Coriolis, and Euler Accelerations

The preceding are associated with the spacecraft attitude motions; i.e., they arise from the nature of the rotation of the spacecraft frame of reference to the geocentric inertial frame.[3,4] For the inertial attitude considered in this work these relative accelerations are zero, while for the radial attitude motion they are not. The Euler accelerations arise from the rate of change of angular velocity of the spacecraft. For a spacecraft subject to atmospheric drag with an osculating eccentricity $e(\theta)$ that is less than 10^{-6}, they can be neglected as a first approximation. At such low eccentricities the orbit is quasicircular, and the combined effect of the gravity gradient and centrifugal acceleration yields a relative acceleration, given by

$$\begin{bmatrix} 3 & 0 & 0 \\ 0 & -1 & 0 \\ 0 & 0 & 0 \end{bmatrix} \begin{bmatrix} X_1 \\ X_2 \\ X_3 \end{bmatrix} \tag{3}$$

which is often mistakenly referred to as the gravity gradient acceleration. In fact, the centrifugal force augments the gravity gradient acceleration in the local vertical direction (X_1) and cancels the gravity gradient component tangent to the flight path (X_3). Table 2 gives the changes in the latter accelerations per meter from the mass center for different altitudes of the spacecraft mass center. In addition to the centrifugal and Euler accelerations, there will also be Coriolis accelerations. The latter will be significant for particles moving in a vacuum or a low-viscosity fluid.[3-6]

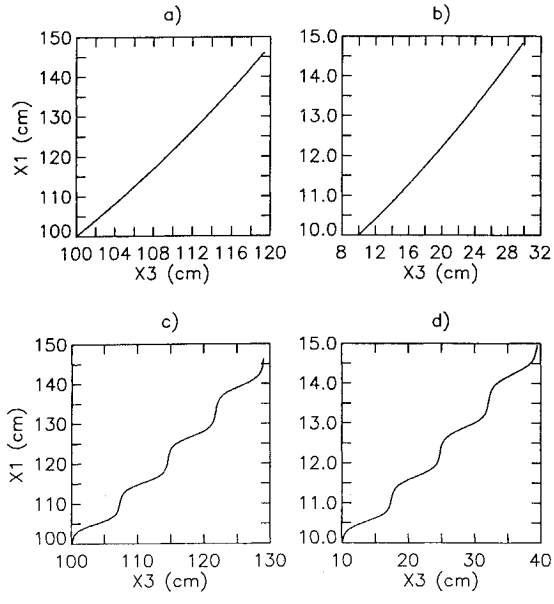

Fig. 2 Particle trajectories as seen by an observer in the spacecraft frame in a radial attitude motion. The origin is the spacecraft mass center. Initial conditions: a) $x_K = (100, 0, 100)$ cm, $\dot{x}_K = 0$, $e(0) = 10^{-6}$; b) $x_K = (10, 0, 10)$ cm, $\dot{x}_K = 0$, $e(0) = 10^{-6}$; c) $x_K = (100, 0, 100)$ cm, $\dot{x}_K = 0$, $e(0) = 0.01$; d) $x_K = (10, 0, 10)$ cm, $\dot{x}_K = 0$, $e(0) = 0.01$.

Table 2 Changes in the X_1 and X_2 acceleration components (in μg/m from the mass center of the spacecraft) associated with the radial attitude

Altitude, km	X_1	X_2
275	0.414	−0.137
300	0.41	−0.136
325	0.405	−0.134
350	0.401	−0.133
375	0.396	−0.131
400	0.392	−0.13
425	0.388	−0.128
450	0.383	−0.127
500	0.375	−0.124
525	0.371	−0.123
550	0.367	−0.121
575	0.363	−0.12
600	0.359	−0.119

Table 3 Estimates of upper and lower atmospheric drag acceleration levels

Altitude, km	Acceleration, μg			
$\bar{\beta}$, cm^2-g^{-1}	0.059[a]	0.01[a]	0.3[b]	0.09[b]
275	2.1	0.36	10.6	3.1
300	1.2	0.21	6.1	1.8
325	0.69	0.12	3.6	1.1
350	0.41	0.07	2.1	0.6
400	0.24	0.025	0.7	0.2
450	0.05	0.009	0.4	0.1
500	0.02	0.001	0.8	0.02

[a]Shuttle.[12] [b]Space Station.

Stokes' Motion Driven by Microgravitational Accelerations

The acceleration, relative to the experimental frame experienced by a spherical particle immersed in a linear viscous fluid of the particle, is given by[3,6]

$$\ddot{x}_\alpha = \delta F^{(b)}_\alpha - S\dot{x}_\alpha \tag{4}$$

where δ is the buoyancy coefficient, which includes the effects of added mass,[10,11]; S is the dimensionless Stokes' coefficient; and $F^{(b)}_\alpha$ is the effective buoyancy force.[12] $F^{(b)}_\alpha$ is given by

$$\begin{aligned} F^{(b)}_\alpha &= \left(\dot{Q}_{\alpha\beta} + Q_{\alpha\gamma}Q_{\beta\gamma}\right) x_\beta + 2Q_{\alpha\beta}\dot{x}_\beta \\ &+ R_{\alpha K}\left[2\Omega_{KM}R_{\beta M}\dot{x}_\beta + \left(\Omega_{KP}\Omega_{MP} + \dot{\Omega}_{KM}\right) R_{\beta M}\left(x_\beta - p_\beta\right)\right] \\ &+ G_{\alpha\beta}\left(x_\beta - p_\beta\right) + R_{\alpha K}A_{KK^*}F^D_{K^*} \end{aligned} \tag{5}$$

where $Q_{\alpha\beta}$ and Ω_{KM} are skew tensors, which represent the rates of rotation of the experimental frame with respect to the spacecraft frame and the rate of rotation of the spacecraft frame with respect to the geocentric inertial frame. It is implicit in the preceding equations that the history integral, which appears in the Basset-Boussinesque-Oseen equations,[10,11,13] has been neglected as well as the influence of rigid walls which contain the fluid.

The preceding equations together with the initial conditions

$$\dot{x}_\alpha = 0, \quad x_\alpha = x^0_\alpha \tag{6}$$

have been solved numerically for various values of the parameters S and δ, and for different rotations of the experimental system relative to the spacecraft. It should be noted that, in general, because of atmospheric drag effects, the osculating elements of the orbit, a, e, and $\bar{\omega}$, must be found as functions

of time[5,8,9] [or the angular position, $\theta(t)$, of the spacecraft]. The calculations were carried out using dimensionless drag coefficients that correspond to estimated drag coefficients for the Shuttle and the Space Station, and for typical orbital altitudes: on the order of 300 km for the Shuttle and 500 km for the Space Station.

Results

The physical parameters S and δ lie in the ranges $0 \leq S \leq \infty$ and $-\infty < \delta \leq 1$, respectively. In the extreme case $S = 0$, $\delta = 1$ represents a drag-free particle,[3,4] while $S = \infty$ corresponds to a rigid solid. Herein, the calculations are restricted to the ranges $20 \leq S \leq 1200$ and $-1 < \delta < 1$. Selected examples of the authors' results are illustrated in Figs. 2–6 and Table 4. For the figures, all calculations were undertaken for four Earth orbits (approximately 6h) and with $\bar{\beta} = 0.01$, $a_0 = 6688$ km, $S = 100$, and $\delta = 0.5$.

Figures 2 and 3 illustrate the effect of spacecraft attitude motions on the trajectory of the particle, for the radial and inertial attitudes, respectively (the experimental frame is coincident with the spacecraft frame). Notice that for a given attitude the extent of the motion depends on the initial distance of the particle from the mass center, the buoyancy δ,[3] and Stokes' drag S.[3,4] The nature of these trajectories can be understood by using Tables 1–3, and upon inspection of Eq. (5) with $Q_{\alpha\beta} = \dot{Q}_{\alpha\beta} = 0$. For the radial mode, the initial acceleration experienced by the particle is obtained from Eq. (5), with Ω_{KM} given by

$$\Omega_{KM} = \dot{\theta}\begin{bmatrix} 0 & 0 & 1 \\ 0 & 0 & 0 \\ -1 & 0 & 0 \end{bmatrix} \tag{7}$$

where $\dot{\theta}$ is calculated from the osculating elements[3,8] $a(\theta)$, $e(\theta)$, and $\bar{\omega}(\theta)$.

As mentioned earlier, the gravity gradient force per unit mass felt by the particle parallel to X_1 is augmented by the centrifugal force. This component of acceleration is given approximately by

$$a_1 \simeq 3\left(\gamma/\alpha_0^3\right) X_1 \tag{8}$$

The X_3 gravity gradient component is approximately canceled, leaving only the drag force and the Coriolis force acting in this direction. From Table 2, it can be seen that a_1 increases a distance of approximately 0.41 μg/m from the center of mass (for a mass center altitude of 275 km). When the initial X_1 position of the particle is within 1 m of the mass center of the spacecraft, the accelerations resulting from the atmospheric drag dominate and the particle moves a greater distance along the X_3 axis. For the drag coefficient ($\bar{\beta} = 1.02 \times 10^{-2}$) used here, and for initial X_1 positions greater than 1 m, the combined effects of the gravity gradient and centrifugal force begin to compete with the atmospheric drag term and eventually dominate. As the particle velocity increases, so does the effect of the Coriolis force. This becomes evident at lower values of S (nondimensional Stokes' coefficient) and larger density differences. The trajectories calculated for the inertial attitude illustrate the nature of the gravity gradient force. For the radial attitude, the gravity gradient tensor can be written as

$$G_{KM} = \frac{1}{r_0^3}\begin{bmatrix} 2 & 0 & 0 \\ 0 & -1 & 0 \\ 0 & 0 & -1 \end{bmatrix} \tag{9}$$

while for the inertial attitude it takes the form

$$G_{KM} = \frac{1}{r_0^3}\begin{bmatrix} 3\cos^2\theta - 1 & 0 & 3\cos\theta\sin\theta \\ 0 & -1 & 0 \\ 3\cos\theta\sin\theta & 0 & 3\sin^2\theta - 1 \end{bmatrix} \tag{10}$$

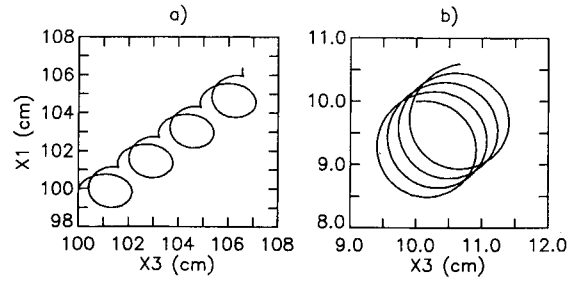

Fig. 3 Particle trajectories as seen by an observer in the spacecraft frame in an inertial attitude motion. The origin is the spacecraft mass center. The initial conditions are: a) $x_K = (100, 0, 100)$ cm, $\dot{x}_K = 0$, $e(0) = 10^{-6}$; b) $x_K = (10, 0, 10)$ cm, $\dot{x}_K = 0$, $e(0) = 10^{-6}$.

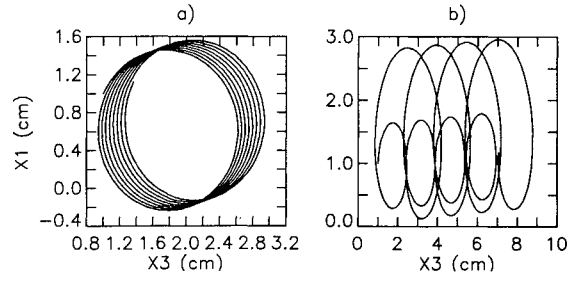

Fig. 4 Particle trajectories as seen by an observer in the experimental frame. a) $-2.0\ \omega_0$, $e(0) = 10^{-6}$; b) $-2.0\ \omega_0$, $e(0) = 0.01$.

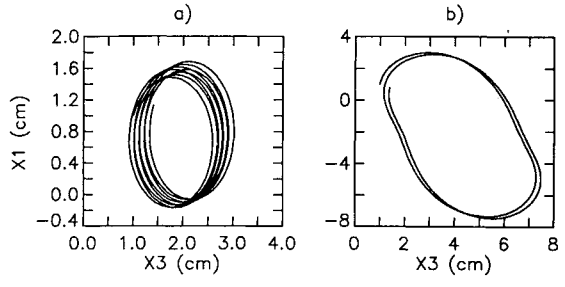

Fig. 5 Particle trajectories as seen by an observer in the experimental frame. a) $-2.0\ \omega_0$, $e(0) = 10^{-3}$; b) $-0.5\ \omega_0$, $e(0) = 0.01$.

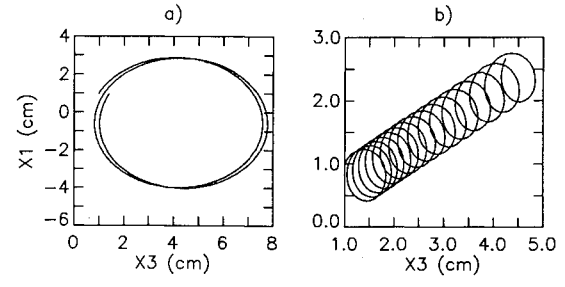

Fig. 6 Particle trajectories as seen by an observer in the experimental frame. a) $-0.5\ \omega_0$, $e(0) = 10^{-6}$; b) $-4.0\ \omega_0$, $e(0) = 10^{-6}$.

The calculated trajectories in Fig. 2 also illustrate the effect of $e(\theta)$, the osculating eccentricity. Figures 2c and 2d show fluctuations that have, approximately, the frequency ω_0. Because of the relativity large value of $e(0)$, the spacecraft passes through regions of relatively high and low atmospheric density during one orbit. During the time the spacecraft is traveling through a relatively low density atmosphere, the drag acceleration experienced by the particle decreases and the gradient dX_1/dX_3 increases; in high-density areas, the drag acceleration decreases, resulting in a perturbation that favors the

Table 4 Maximum displacement from initial position during two orbits

S	δ	ω_e	ΔX_{max}, cm
20	0.8	0	354
20	0.5	0	163
20	0.8	$-2\omega_0$	20
20	0.5	$-2\omega_0$	11
10^2	0.8	0	38
10^2	0.8	$-2\omega_0$	1.80
10^3	0.8	0	3.35
10^3	0.5	0	2.24
10^3	0.5	$-2\omega_0$	0.16
10^3	0.5	$-4\omega_0$	0.14

component of motion parallel to X_3 rather than X_1 (i.e., dX_1/dX_3 decreases).

The trajectory in Fig. 3a is associated with an initial position of (10, 0, 10) cm from the spacecraft mass center. In this region, atmospheric drag effects predominate. Thus the gravity gradient acceleration is masked by the drag acceleration, which has the same frequency[3,6] as the orbit of the spacecraft around the Earth. At an initial position of (100, 0, 100) cm from the mass center, however, the atmospheric drag acceleration no longer masks the effect of the gravity gradient acceleration. The resulting trajectory reflects the fact that the frequency of the gravity gradient acceleration is twice that of the orbital frequency.

Figures 4–6 illustrate some examples of calculations for which the experimental frame was rotated relative to the spacecraft frame. In each case, the particles are initially at rest; i.e., $\dot{x}_\alpha = 0$, and the initial position was taken to be $x_\alpha = (1, 0, 1)$ cm. Each trajectory is shown as seen by an observer in the experimental frame of reference. The origin of the experimental frame was taken to be at a position $X_K =$ (100, 0, 100) cm. The axis of rotation passed through the origin of the experimental frame of reference and was oriented perpendicular to the orbital plane. The spacecraft frame is undergoing a basic rotation (relative to the geocentric inertial frame) about an axis perpendicular to the orbital plane. We emphasize at this stage that if the rotation axis of the experimental frame relative to the spacecraft frame is not exactly parallel to the basic rotation axis of the spacecraft frame, there will be precessional stirring of the fluid.[14,15] If the sine of the angle between these axes becomes too large, the "spin-up" assumption invoked in the derivation of Eq. (5) will no longer be reasonable. The motion of the stirred fluid will affect the motion of the particle.

Table 4 shows the effect of varying the parameters S, δ, and ω_e on the maximum displacement from the initial position that occurred during two orbits. The initial position in the experimental frame was (1, 0, 1) cm.

As expected, the effect of either increasing S or decreasing δ is to reduce the maximum displacement ΔX_{max} from the initial position. While $-2\omega_0$ was not always the most effective rate of rotation for short times (one or two orbits), it was most effective over longer times (four or more orbits).

Conclusions

The effects of the residual acceleration associated with the gravity gradient, centrifugal acceleration, Euler acceleration, and the atmospheric drag force on the motion of a solid spherical particle in a viscous fluid have been demonstrated. For experiments involving suspensions of particles, it may be desirable to increase the residence time of a particle in a given region of the host liquid (for example, to delay sedimentation onto the container walls bounding the liquid). Under the assumption that spin-up of the fluid can be achieved in a reasonably short time, and that the local axis of rotation is exactly parallel to the basic rotation axis of the spacecraft relative to the geocentric inertial frame, it has been demonstrated that the residence time of a spherical particle in a given region of the fluid can be increased substantially by an appropriate rotation of the experimental frame relative to the spacecraft frame. The most effective choices of rotation appear to be twice and one-half the angular speed of the spacecraft. The best was at twice the orbital rate and in the opposite sense to the direction of motion of the spacecraft.

In this work, attention has been confined to particles that lie in the orbital plane of the spacecraft. A discussion of more general initial conditions can be found elsewhere.[5]

In addition to examination of Stokes' motion, "rule of thumb" estimates of residual accelerations arising from the gravity gradient, attitude motions, and atmospheric drag have been tabulated (see Tables 1–3). The effect of altitude on the acceleration fields caused by the spacecraft attitude and the gravity gradient can be summarized as follows: for a range of altitudes that typify Shuttle and anticipated Space Station orbits, the decrease in the magnitude of the accelerations per 100-km change in the altitude of the spacecraft mass center is approximately 6 ng for the X_2 component and 18 ng for the X_1 component (when the craft has a radial attitude motion). The effect of altitude changes on the acceleration produced by atmospheric drag is more severe. For a given drag coefficient β, the change in the mean atmospheric density associated with a 100-km altitude change results in an order-of-magnitude change in the drag acceleration (see Table 3).

It is readily concluded that, for experiments insensitive to "steady" accelerations below 1 μg, a substantial increase in the orbital altitude is worthwhile only if the effect of atmospheric drag can be reduced. Space Station orbits will be at much higher altitudes than those typically associated with the Shuttle. Therefore, it might be expected that, as a result, the drag acceleration experienced by the Space Station will be lower. However, the diminishing effect of the greater altitude will be slightly offset by the fact that the Space Station has a higher surface area-to-mass ratio than the Shuttle, and thus experiences more drag at a given altitude.

For those experiments sensitive to accelerations below 1 ng increased altitude is clearly desirable. However, this may be effective only if drag effects can be reduced. The latter may be affected either by continuous "drag makeup"[16] or by launching free-flying modules with low aerodynamic drag characteristics.

Acknowledgments

The first author would like to acknowledge support provided through the USRA Visiting Scientist program. The authors also wish to acknowledge the stimulating comments of an anonymous reviewer.

References

[1] Langbein, D., "Allowable G-levels for Microgravity Payloads," *European Space Agency Journal*, to be published, 1986.

[2] Kamotani, Y., Prasad, A., and Ostrach, S., "Thermal Convection in an Enclosure due to Vibrations Aboard a Spacecraft," *AIAA Journal*, Vol. 19, 1981, pp. 511–516.

[3] Alexander, J.I.D. and Lundquist, C.A., "Residual Motions Caused by Microgravitational Accelerations," MSFC Space Science Lab., Preprint Series No. 86-132, 1986, see also, *Journal of the Astronautical Sciences*, to be published, 1987.

[4] Bauer, H.F., "Motion Trajectories of Particles Inside and Outside an Orbiting Space Shuttle," *Zeitschrift für Flugwissenchaften und Weltraumforschung*, Vol. 10, 1986, pp. 22–33.

[5] Alexander, J.I.D., NASA Technical Memorandum, in preparation.

[6] Lundquist, C.A., "Attitude Control for Experiments in Microgravity," *AIAA Guidance and Control Conference Proceedings*, 1983, pp. 665–668.

[7] Forward, R.L., "Flattening Space-Time Near the Earth," *Physical Rev. D*, 26, 1982, pp. 735–744.

[8]Sterne, T.E., *An Introduction to Celestial Mechanics*, Interscience, New York, 1960.

[9]King-Hele, D., *Theory of Satellite Orbits*, Butterworths, London, 1964.

[10]Monti, R., *G-Level Threshold Determination*, Techno-Systems Rept. TS-7-84, Techno-Systems Developments, Napoli, Italy, 1984.

[11]Basset, A.B., *A Treatise on Hydrodynamics*, Vol. 2, Dover, New York, 1961.

[12]Mullins, L., *Aerodynamic Design Databook, Vol. I, Orbiter Vehicle*, SD-732-SH-0060-1K, Rockwell International, 1977.

[13]Batchelor, G.K., *Fluid Dynamics*, Cambridge University Press, London, 1967.

[14]Malkus, W.V.R., "Precession of the Earth as the Cause of Geomagnetism," *Science*, Vol. 160, 1968, p. 259.

[15]Gans, R.F., "On Precession of a Reasonant Cylinder," *Journal of Fluid Mechanics*, Vol. 41, 1970, p. 865.

[16]Garriot, O.K., personal communication, Guntersville, AL, 1986.